Meas. Sci. Technol. 1 (1990) 1363–1370. Printed in the UK

Optimization and characterization of a differential photopyroelectric spectrometer

Constantinos Christofides, Kamyar Ghandi and Andreas Mandelis

Photoacoustic and Photothermal Sciences Laboratory, Department of Mechanical Engineering, and Ontario Laser and Lightwave Research Center, University of Toronto, Toronto, Ontario, Canada M5S 1A4

Received 18 April 1990, in final form 12 July 1990

Abstract. A differential photopyroelectric (P^2E) spectrometer using thin pyroelectric PVDF film, with real-time spectrum normalization measurement capability has been recently developed and characterized. The spectrometer is able to perform measurements as a function of wavelength (limited by the Xe lamp spectrum: 280–1960 nm) and modulation frequency (0.1–600 Hz). The aim of this paper is to describe the abilities and advantages of the photopyroelectric spectrometer over other photothermal spectroscopic instrumentation, and to draw attention to different sources of possible experimental errors. Several experiments have been performed as a function of wavelength and/or modulation frequency in order to calibrate, characterize and optimize the working conditions of the photopyroelectric spectrometer. Some further measurements on c-Si have been performed in order to show the instrumentation capabilities. The present differential photopyroelectric spectroscopic technique seems to be very promising toward the characterization of semiconductor thin films and devices.

1. Introduction and background

In this paper we will describe and characterize a new differential real-time-normalizing photopyroelectric (P^2E) spectrometer and will discuss its performance in the infrared spectral range (600–1400 nm), including some experimental results on c-Si. The analysis of photopyroelectric measurements on crystalline silicon (pure and extrinsic) will be presented elsewhere (Christofides *et al* 1990a).

The aim of this paper is to present some key experiments for the characterization and the calibration of the spectrometer and to show the capabilities, advantages and disadvantages of the photopyroelectric spectroscopic technique as it becomes a valuable tool for non-destructive evaluation (NDE) of materials (Christofides *et al* 1990a, b, Coufal and Mandelis 1987, Mandelis *et al* 1989). In this paper, we also present progress on the development of the spectrometer, as well as various problems and limitations that have appeared during the instrumental evolution and optimization.

As is well known, the limitations of conventional optical spectroscopies (Rosencwaig 1980, Bosquet 1971) led to the development of new spectroscopic techniques, including those in the photothermal family. In fact, the last half century shows that the conventional spectroscopies could not give satisfactory results especially in the case of (i) highly transparent materials (such as crystalline materials and gases), due to the fact that these materials do not efficiently attenuate the transmitted beam, and (ii) materials with high absorption coefficient, due to the inability for transmission spectroscopic analysis (Rosencwaig 1980). Over the years, several techniques have been invented in order to give some viable solution to this problem. Among others, one can distinguish diffuse reflectance (Wendlandt and Hecht 1966), attenuated total reflection, internal reflection spectroscopy (Wilks and Hirschfeld 1968) and Raman spectroscopy (Wright 1969). These techniques have been found very useful; however, the classes and types of materials that can be used with each are limited due to the short range of useful wavelengths.

This important impediment was substantially alleviated with the introduction of the modern version of photoacoustic spectroscopy (PAS) (Rosencwaig 1973). The main difference between PAS and the earlier photonic techniques mentioned above, lies in the fact that with PAS one can analyse the light–sample interaction not through the detection of some photons, but through the energy absorbed and converted into heat by the material, via non-radiative processes. PAS is not only an optical spectroscopic technique, but also a form of calorimetry with advantages over other conventional calorimetric methods, such as high sensitivity and fast response. PAS has been found to present two major advantages: (i) The generated photoacoustic signal is relatively insensitive to

0957-0233/90/121363+08 $03.50

transmitted or elastically scattered photons. This advantage increases the capabilities of the method in the case of weakly absorbing samples (Rosencwaig 1980) and has made the technique an excellent tool for the spectroscopic characterization of gases. (ii) The photoacoustic signal exists even in the case of highly absorbing materials or completely opaque materials. This capability of PAS led to spectroscopic applications towards the photoacoustic characterization of semiconducting materials.

Photopyroelectric spectroscopy (P^2ES) is a related technique, with which this paper deals exclusively. The former PAS advantage presented above is not pertinent in the case of P^2ES. In fact, with P^2ES the transmitted light generates a strong pyroelectric signal; however, this contribution is, within some limits, easy to distinguish from the signal contribution due to the absorption of light in the sample itself. On the other hand, P^2ES is technically less complex and less expensive than PAS: instead of a microphone, a pyroelectric thin film is necessary. Like PAS, P^2ES also has the useful capability of performing non-destructive evaluation (NDE) and depth-profile analysis of the light absorption in a material. One disadvantage of P^2ES, as well as for the PAS technique, is susceptibility to synchronous acoustic noise. For both techniques this problem can be partially alleviated by isolation of the mechanical chopping system from the optical table which supports the rest of the instrumentation, or the use of acousto-optic or electro-optic modulation schemes, when laser excitation is feasible.

The first measurements of the pyroelectric effect, which was discovered 300 years ago, appeared shortly before World War I (Roentgen 1914, Ackerman 1916). The first use of pyroelectric sensors for the detection of infrared radiation was reported by Yeou (1938). However, almost 30 years passed before the first practical applications of a pyroelectric detector were reported (Beerman 1967). In 1984 Coufal (1984a) and Mandelis (1984) used, for the first time, thin pyroelectric polyvinylidene fluoride (PVDF) films for photothermal-wave based spectroscopic detection. Shortly after, Coufal showed that photopyroelectric spectroscopy can be a very sensitive qualitative tool for thin film spectroscopic applications (Coufal 1984b). Tanaka (1987) and Tanaka *et al* (1988) showed that frequency-domain P^2ES is also very promising for quantitative analysis.

Recently, P^2ES has been used for the characterization of thin semiconducting films. Mandelis *et al* (1989) have performed spectroscopic measurements of an a-Si:H thin film on quartz. These authors further compared their experimental P^2E spectra with similar spectra obtained by conventional, widely used photothermal deflection spectroscopy (PDS). This comparison showed comparable performance of P^2ES as an absorption spectrum-determining quantitative technique. Furthermore, it was shown that P^2ES has the ability for easy and self-consistent experimental acquisition of non-radiative quantum efficiency spectra, a property not shared by PDS. PDS has other limitations, such as the requirement for a coupling fluid (usually carbon tetrachloride) which has a large refractive index gradient with respect to temperature change, and low absorption coefficient. This liquid medium may alter the surface characteristics of the sample under investigation, especially where delicate ultrathin, electronically active surfaces are concerned. According to Amer and Jackson (1984) there is evidence to suggest that carbon tetrachloride, specifically, does not alter the properties of a-Si:H films. Nonetheless, a system with no coupling fluid would eliminate the possibility of sample property alteration or surface contamination for some materials. It is the necessity for a coupling fluid that is partly the cause of the lack of spectroscopic applications of PDS at cryogenic temperatures. Another disadvantage is the pump–probe beam alignment requirement for PDS detection. This frequently leads to the need for three-dimensional models in order to interpret the data quantitatively. The consideration of these disadvantages led to the development of P^2ES in this laboratory. Very recently, Christofides *et al* used P^2ES for spectroscopic measurements on crystalline Ge (Christofides *et al* 1990b) and Si (Christofides *et al* 1990a). Those preliminary measurements led the present authors to search for a more sensitive version of the P^2E instrumentation, with higher reproducibility and signal-to-noise ratio (SNR) than the original single-ended technique (Mandelis 1984).

In section 2 of this paper, the instrumentation for differential P^2ES will be discussed in detail. Several experiments will be presented as a function of modulation frequency and/or wavelength and the P^2E response will be discussed. Finally, the use of the photopyroelectric spectrometer for spectroscopic measurements on pure crystalline silicon samples will be described.

2. Instrumentation

2.1. Experimental set-up

Figure 1 presents the experimental set-up of P^2ES for a differential or real-time normalizing mode. White light from a 1000 W Xe lamp was passed through an ISA monochromator (model H-20) which housed an infrared-blazed grating, adjustable through a stepping motor (step motor 2 in figure 1) under IBM PS/2 computer control, to produce an automated wavelength scanning system. A broad range of slits was available and was used with this spectrometer, allowing the spectral resolutions of 16, 8 and 4 nm, respectively. The spectral cut-off filters associated with the monochromator were changed automatically at three different wavelengths (750, 860 and 1300 nm), using an electromechanical solenoid switch. Three filters have been used in the P^2E instrumentation in order to provide light in the widest possible wavelength range permitted by the spectral throughput of the lamp (270–190 nm). Two experimental configurations were used to allow spectroscopic measurements in a wide range of modulation frequencies. Using an oscillating mirror (M) the swept beam was focused alternately on two spots on a plane where the active elements of two photopyroelectric detectors were placed. At those spots the beam sizes were approximately $1 \times 0.5\ mm^2$ each. A

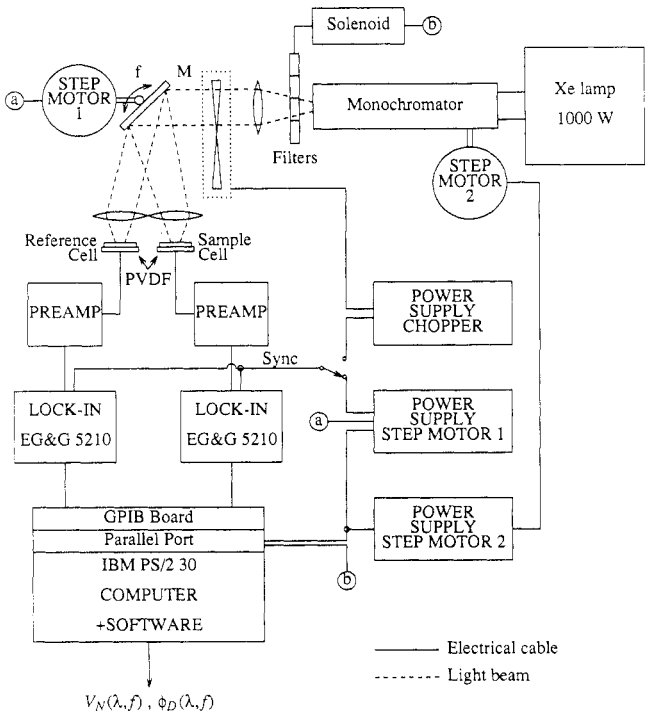

Figure 1. Dual-channel photopyroelectric spectrometer instrumentation.

special effort to minimize the size of the illuminated spot was made in order to maximize the irradiance of the incident beam. The mirror was made to oscillate by a stepping motor (step motor 1 in figure 1) in the range of 0.1–15 Hz. The step motor could rotate through more than 400 discrete position steps per second in the clockwise direction. For counterclockwise oscillations the step-motor was limited to only 15 steps per second. This limitation is the reason why a chopping motor was required for frequencies higher than 15 Hz. Figure 2 presents a schematic diagram of this component at low frequency operation (0.1–15 Hz). This modulation method is preferable to a beam-splitter/mechanical-chopper arrangement, since it avoids the wavelength dependence of such optics. For frequencies in the 15–600 Hz range, an EG&G chopper (model 192) was placed before the mirror to provide the modulation while the mirror was controlled by the computer to switch from the sample to the reference detector after a measurement at each wavelength was made. In figure 3 we present a schematic diagram of the modulation component at high modulation frequencies (15–600 Hz). In this mode, the data acquisition software ensured that any intensity variation of the lamp during successive measurements of sample and reference did not contribute a considerable error. It is important to note that the two Al–Ni–PVDF photopyroelectric detectors were covered with black paint in order to absorb maximum optical flux of the same amplitude and eliminate reflected light contribution throughout the entire spectrum (black bodies). However, black painted PVDF films introduce some variations in the signal output from the two films because it is very difficult to obtain exactly the same paint thickness. This thickness was maintained as low as possible in order to avoid the introduction of thermal characteristics of the paint in the signal generation mechanism. The two output signals were bandpass-filtered and preamplified by two low-noise Ithaco preamplifiers (model 1201). They were then connected to a double-input Tektronix (model T912) oscilloscope for visual display, and to two digital two-channel EG&G (model 5210) lock-in analysers (see figure 1). Depending on the configuration used, the reference for the lock-ins was obtained either from the oscillating mirror (0.1–15 Hz) or from the chopper (15–600 Hz). For very low frequencies (0.5–0.1 Hz) the signal was detected and measured directly by the computer through an analogue-to-digital converter. An IBM computer equipped with a mathematical co-processor for fast calculations interacted with the two lock-in outputs through a GPIB board, and calculated amplitudes and phases. At the same time, the software graphics displayed the photopyroelectric normalized voltage and phase difference as a function of the frequency or wavelength on the split screen. Using only the two black PVDF films the normalized magnitude signal V_N was further calibrated ($V_N \rightarrow 1$) at the beginning of each experiment by a judicious choice of gain on the Ithaco low-noise preamplifiers. Ideally the phase difference of the two detectors is close to 180 degrees in the case of the configuration presented in figure 2 where the modulated mirror (M) sweeps across the two sensors, and close to zero degrees when the mechanical chopper is modulating the light (see figure 3).

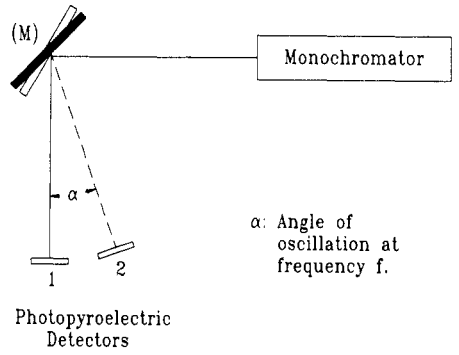

Figure 2. Light–oscillating-mirror–detector arrangement at low modulation frequencies ($0.1 \leqslant f \leqslant 15$ Hz).

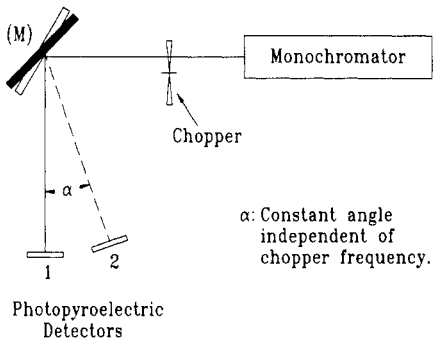

Figure 3. Light–chopper–mirror–detector arrangement at high modulation frequencies ($15 \leqslant f \leqslant 600$ Hz).

2.2. Instrumental optimization concerning light beam intensities

One of the most challenging technical problems dealt with during the development of the photopyroelectric spectrometer was the requirement for equal light beam intensities directed toward the two photopyroelectric detectors. This is a fundamental requirement for differential measurements of optimum sensitivity. Unequal light beam intensities do not have any influence on the phase difference of the photopyroelectric signals produced by the two detectors 1 and 2 (see figures 2 and 3); on the other hand they introduce a considerable error to the ratio of the two photopyroelectric amplitude signals, V_1/V_2. In fact, according to Mandelis and Zver (1985) in the absence of a sample, the P²E signal $V(f)$ generated by a thin-film black-body non-reflecting reference deposited directly on the pyroelectric detector can be written in the form

$$V(f) = A_p \eta_p \frac{pI_0}{2k\varepsilon_0}\left(\frac{1}{k_p \sigma_p^2}\right) \tag{1}$$

where p and k are the pyroelectric coefficient and the dielectric constant of the pyroelectric medium, respectively; I_0 is the light source irradiance incident on the solid surface; ε_0 is the dielectric constant of vacuum (8.85418×10^{-12} C V^{-1} m^{-1}); $\sigma_p = (1+i)\alpha_p$, with α_p the thermal diffusivity of the pyroelectric film and $i^2 = -1$; k_P is the thermal conductivity of the PVDF, and η_p is the non-radiative conversion efficiency (or heat conversion efficiency) for the black-body pyroelectric film. From equation (1) one can write the ratio V_1/V_2 as

$$V_N = \frac{V_1}{V_2} = \frac{I_{01}}{I_{02}} \tag{2}$$

where I_{01} and I_{02} are the amplitudes of the light intensity directed to the two photopyroelectric detectors 1 and 2, respectively. It is obvious from equation (2) that unequal intensities will introduce an error to the amplitude ratio of the two photopyroelectric signals. If we assume

$$I_{01} = I_{02} + \delta I \qquad \delta I \ll I_{02} \tag{3a}$$

equation (2) can then be written as

$$V_N = 1 + (\delta I / I_{02}). \tag{3b}$$

We note that an x% difference in the light beam intensity introduces an (x/I_{02})% error in the amplitude ratio. It has been found that for high accuracy differential measurements, even 1% error introduces significant distortion of the experimental differential results. For example, it would be problematic to make differential spectroscopic measurements between c-Si and lightly implanted c-Si, where the difference in optical absorption coefficient is less than 1%.

In order to resolve the unequal intensity problem, we closely examined some possibilities of technical improvement towards the greatest possible reduction of δI. The step-motor was found to give chopped illumination with optimum control of frequency and amplitude of beam oscillation.

Furthermore, the two beams passed through the same optical paths, i.e. the same filters and lens optics. The mirror (M) (see figures 1, 2 and 3) was coated with a silver coating, in order to have high average reflectance (98%) (Melles-Griot 1988) in the wavelength range 400 nm to IR. The angle α (see figure 3) was taken as small as possible in order to avoid any possible difference in reflectance due to the angle of incidence. The minimization of the angle α was the key to optimizing the spectrometer. This was accomplished by moving the detectors as far as possible from the mirror in order to keep the angle α as small as possible.

Another important matter that was taken into account was the choice of an optical network (filters, lenses, mirror) with very limited attenuation in the infrared region, especially in the wavelength range 1600–1960 nm where the throughput of the Xe lamp is very low (30 to 40 times lower than in the visible region). The weakness of the Xe lamp in that spectral region created some experimental problems for the present authors, with respect to the S/N ratio during the characterization of crystalline Ge (bandgap close to 1800 nm (Christofides *et al* 1990b)). The necessity of using minimum attenuation lenses and maximum reflectance mirrors was a fundamental concern during the development of the spectrometer for infrared applications.

3. Photopyroelectric spectroscopic characterization

3.1. Frequency response characterization

For this study two different thicknesses of PVDF were used, 28 and 52 μm, in order to obtain thermally thick photopyroelectric conditions (Mandelis and Zver 1985). The thickness of the PVDF and the modulation frequency must be such that the condition

$$f \gg f_c \equiv \frac{\alpha_p}{\pi L_p^2} \tag{4}$$

is satisfied, according to the definition of the thermally thick limit. α_p and L_p are the thermal diffusivity and the thickness of the pyroelectric film respectively. In equation (4) f_c, the critical frequency, is equal to 22 and 5 Hz, for PVDF thicknesses of 28 and 52 μm, respectively. As is well known (Kynar 1983), the thermal time response of the PVDF film depends on its thickness, yet for our range of frequencies (0.1–600 Hz) this dependence is insignificant. Our frequency response characterization experiments further led to the conclusion that it is necessary to work in a frequency range greater than 5 Hz in order to satisfy the conditions of the theoretical model as expressed by equation (1). Therefore, in all subsequent experimental work, 52 μm thick PVDF was used in order to allow for the largest range of experimental frequencies, as well as to generate high output voltages (Kynar 1983). Figure 4(*a*) shows the variation of P²E voltage as a function of the square root of frequency. One may distinguish two different regimes: the thermally thick and thermally thin regions. The variation of the photopyroelectric

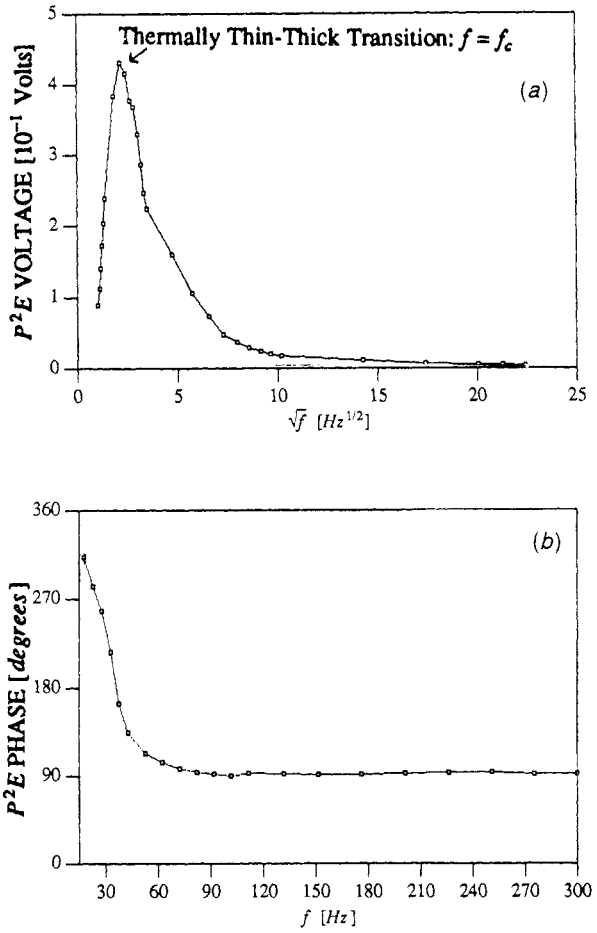

Figure 4. (*a*) Frequency dependence of the black-body–PVDF P^2E voltage amplitude; (*b*) frequency dependence of the black-body–PVDF P^2E phase.

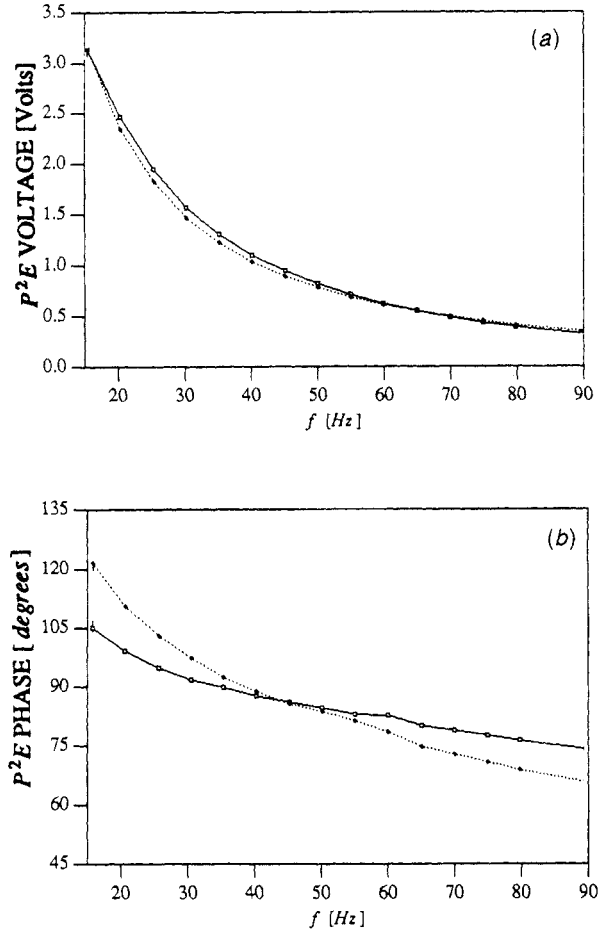

Figure 5. (*a*) Frequency dependence of the P^2E voltages V_1 (full curve) and V_2 (broken curve); (*b*) frequency dependence of the P^2E phases Φ_1 and Φ_2. Excitation source: white light from a 1000 W Xe lamp.

phase against frequency is presented in figure 4(*b*). We note a monotonic behaviour in the thermally thin region of the PVDF film. For frequencies higher than 60 Hz the phase tends to become constant.

In equation (1) one can write the output P^2E voltage amplitude, V, and phase, Φ, from a surface black-body thin film as

$$|V(f)| = \frac{pI_0}{2k\varepsilon_0}\left(\frac{\alpha_p}{2\pi k_p f}\right) \tag{5a}$$

$$\Phi(f) = -\pi/2 \tag{5b}$$

Figures 5(*a*) and (*b*) present plots of the P^2E amplitudes ($|V_1|$ and $|V_2|$) and phases (Φ_1 and Φ_2) as a function of frequency. A ln–ln plot of V against modulation frequency in figure 5(*a*) yields a straight line in the thermally thick region with a slope close to -1 in agreement with equation (5*a*). On the other hand, the phases Φ_1 and Φ_2, in figure 5(*b*) tend to saturation for frequencies greater than 60 Hz, in agreement with the entirely thermally thick, constant behaviour predicted by equation (5*b*).

3.2. Lamp spectral throughput characterization

During the lamp spectral throughput characterization it was observed that the two PVDF detectors sprayed with black paint responded at low modulation frequencies nearly identically to the Xe lamp illumination. The two responses confirmed that the beams were indeed spectrally similar, and that any apparent differences in intensity could be corrected by judicious choice of gain on the preamplifiers. These preliminary experiments have been performed at various frequencies in the range between 0.1 and 600 Hz. It was shown that the spectrometer gives an excellent and reproducible response for frequencies lower than 275 Hz, while the signal-to-noise ratio (SNR) deteriorated at higher frequencies, due to the decreased light intensity and the introduction of acoustic noise generated by the mechanical chopper.

Figures 6(*a*) and (*b*) present the normalized ratio $V_N \equiv V_1/V_2$ and phase difference $\Phi_D = \Phi_1 - \Phi_2$ as a function of frequency. In the range 15–90 Hz, a variation of V_N is observed. In order to correct for the instrumental phase variation a certain preamplifier gain calibration was required as a function of the working modulation frequency. The variation in black-layer thickness on each PVDF film was found to be responsible for these deviations. One can avoid this problem by depositing a very thin black body on the PVDF surface under a well controlled evaporation method. Figures 7(*a*) and (*b*) present the normalized ratio $V_N \equiv V_1/V_2$ and phase difference

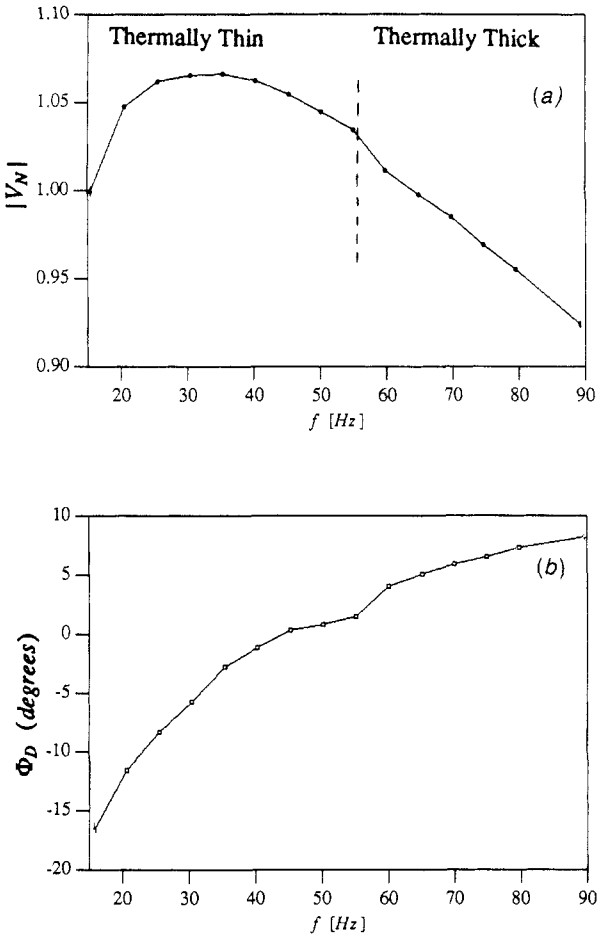

Figure 6. (*a*) Frequency dependence of the P²E normalized voltage V_N; (*b*) frequency dependence of the P²E phase difference, Φ_D. Excitation source: white light from a 1000 W Xe lamp.

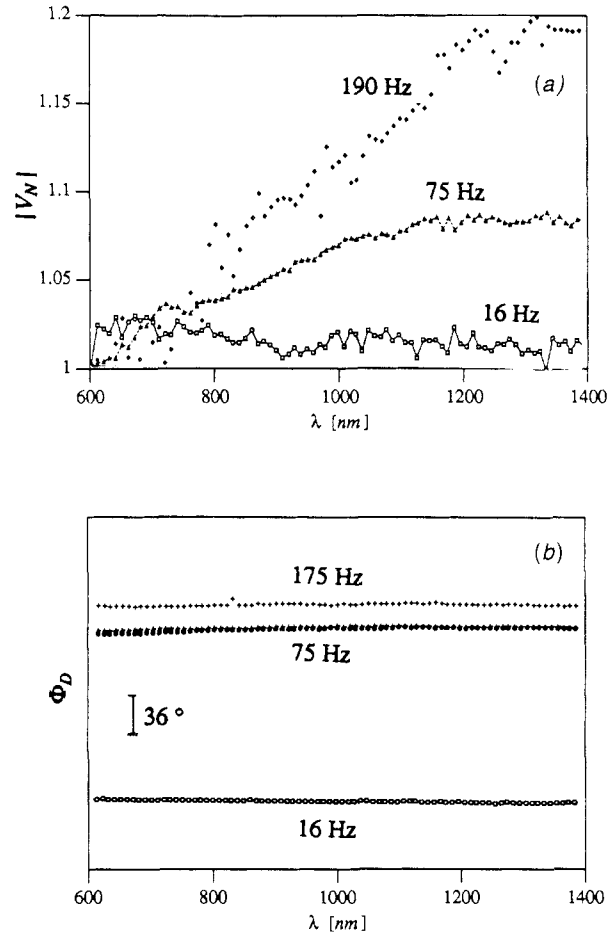

Figure 7. Wavelength dependence of (*a*) P²E normalized signal amplitude $|V_N| = |V_1/V_2|$; (*b*) phase difference $\Phi_D = \Phi_1 - \Phi_2$.

$\Phi_D = \Phi_1 - \Phi_2$ as a function of wavelength. From figure 7(*a*) we note that, at 16 Hz, V_N is almost constant as a function of the wavelength. The normalized signal at 75 Hz, however, presents up to 8% relative deviation between 600 and 1400 nm. The deviation is even higher (close to 20%) at 190 Hz. Although this deviation may seem very large across the entire 600–1400 nm range, it is, in fact, much smaller across practically useful spectral ranges. For example, in the case of spectroscopic measurements on c-Si where the working spectral range lies between 1000 and 1400 nm, the relative deviation is only 1–2% when the modulation frequency is 75 Hz. From figure 7(*b*) we note that Φ_D is completely constant across the wavelengths as expected. The important message of figure 7(*a*) is the necessity of calibration for high precision normalized or differential P²E detection by using such curves, as shown elsewhere (Christofides *et al* 1990a).

4. Spectroscopic measurements on c-Si

The block diagram of the spectrometer has been presented in detail in figure 1. For this study, pure Si samples with crystalline orientation (100) were used. The samples themselves were squares of dimensions 4 × 4 mm² and their thicknesses were 400 μm. The samples were placed on the detector '1' and a gentle pressure was applied in order to obtain good PVDF–sample contact. Optical measurements were subsequently performed across the bandgap of Si (1.12 eV at room temperature) in the range 1000–1400 nm.

Figure 8(*a*) shows normalized P²E spectra of a Si crystal obtained at various frequencies between 15 and 275 Hz at room temperature. As was expected from the transmission-like nature of P²Es near and below the bandgap at high frequencies (Mandelis and Zver 1985), the normalized signal amplitude increased with increasing wavelength (see figure 8(*a*)). We note that in the transparent region, the signal is higher when the frequency is higher. In figure 8(*b*) we present $\log_{10}|V_N|$ against λ in order to be able to examine the opaque region. In fact, the signal in the transparent region is, in some cases, four orders of magnitude higher than in the opaque region. At low wavelengths and high modulation frequencies the thermally thick normalized voltage is very small because it depends mostly on the exponentially decaying thermal contribution. On the other hand, at low modulation frequencies the normalized signal changes less as a function

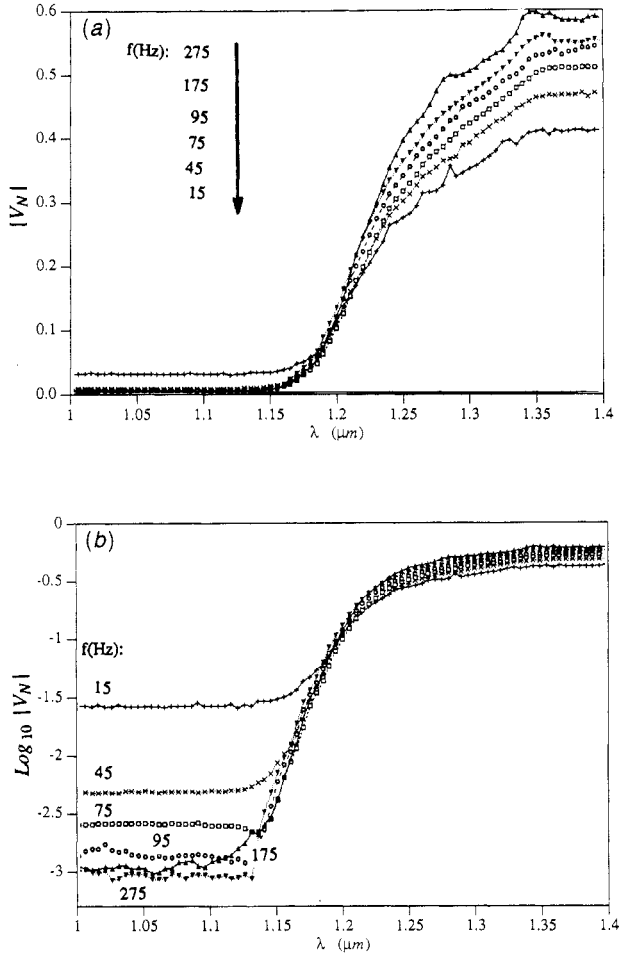

Figure 8. (*a*) P²E normalized voltage spectra of c-Si at various frequencies (resolution 16 nm); (*b*) logarithmic P²E normalized voltage $|V_N|$ spectra of c-Si at various frequencies (resolution 16 nm).

of the wavelength, thus indicating a certain compensation between the thermal and direct optical transmission contributions across the material bandgap.

Figure 9 shows the phase difference Φ_D as a function of the wavelength, λ, for various frequencies at room temperature. These results have been obtained simul-

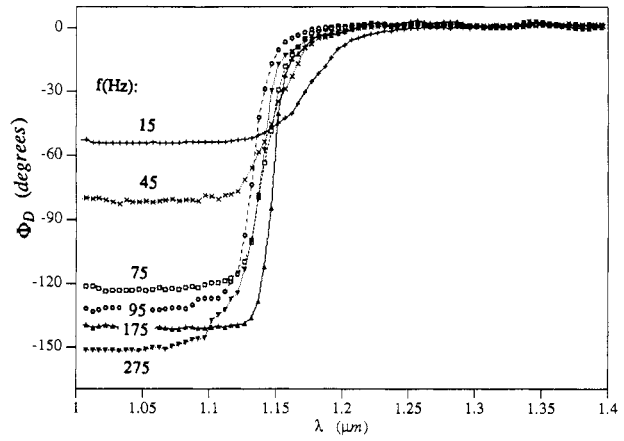

Figure 9. P²E differential phase spectra, Φ_D, of c-Si (resolution 16 nm).

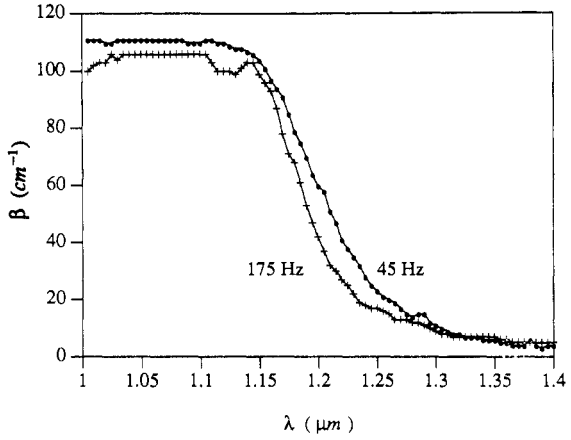

Figure 10. Optical absorption coefficient, $\beta(\lambda)$, spectra for c-Si at two different frequencies.

taneously with the data presented in figure 8(*a*). The following remarks can be made. (1) As was expected in the case of high modulation frequencies, when the bandgap region is approached Φ_D increases significantly as a function of wavelength, as the photothermal phase lag decreases due to the combined effects of the heat centroid moving closer to the back-surface detector (Mandelis and Zver 1985) and the direct transmission signal becoming more significant. The latter effect is important at wavelengths where the sample is partially transparent – in other words, near the bandgap. As the modulation frequency is increased, the wavelength at which the 'transmission' signal becomes dominant shifts to lower values, since the absorption-related heat centroid signal is attenuated. This effect is illustrated experimentally in figure 9 as a phase jump occurring at shorter wavelengths when the modulation frequency is increased. (2) At long wavelengths and for all frequencies, the phase difference Φ_D tends to the same values, due to the dominance of the direct transmission signal over the photothermal absorption signal. (3) The absolute phase difference Φ_D is greater at higher frequencies, as expected. The same behaviour has already been observed by Christofides *et al* (1990b) during photopyroelectric spectroscopic measurements on crystalline Ge. (4) In figure 10 we present optical absorption spectra of the c-Si calculated from various curves of figures 8 and 9 and show the long-wavelength spectrum at 45 and 175 Hz. We note an agreement between our experimental results and those obtained by other workers (Kirev 1975).

5. Conclusion

In this work, a new automatic, differential photopyroelectric spectrometer has been characterized, optimized and used to perform spectroscopy of Si wafers. The spectrometer can be an excellent tool for differential or real-time normalized measurements as a function of modulation frequency and/or wavelength, and it can be used to determine spectroscopic properties of semiconducting materials. The main results of our study can be summar-

ized as follows. (1) The dual-channel (real-time normalizing) photopyroelectric spectrometer has been shown to be capable of highly sensitive spectroscopic non-destructive evaluation of semiconductors of arbitrary thickness as a monitor of either optical absorption or transmission. This ability and the absence of the solid–liquid interface, which may complicate or interfere with qualitative and quantitative analysis of spectra (Wagner *et al* 1986), are important advantages over the well established PDS technique in semiconductor spectroscopy, such as semi-conductor wafers, thin films, optoelectronic and photovoltaic materials, multiple quantum wells and laser materials. P^2ES also offers the possibility for electronic defect studies in processed semiconductors: ion implants, diffusion, annealing and amorphous deposition. High sensitivity thermal studies of materials such as pure metals and alloys are possible. Finally the spectrometer can also be used for non-radiative studies of solids (Mandelis *et al* 1989). (2) Calibration of the spectrometer as a function of modulation frequency and wavelength is needed each time the PVDF films are changed. (3) Special attention must be paid during the paint-spraying of the PVDF films, in order to obtain as much similarity in thickness between the two coatings as possible. (4) Simple, direct spectroscopic measurement of the optical absorption spectra of c-Si has been obtained. (5) The operation of the spectrometer is simple and fast; therefore it is possible to obtain high SNR absorption spectra at data rates of more than one point per minute.

Acknowledgments

The support of the Ontario Laser and Lightwave Research Center (OLLRC) and the Natural Sciences and Engineering Research Council of Canada (NSERC), which made this work possible, are gratefully acknowledged.

References

Ackerman W 1916 *Ann. Phys., Lpz.* **46** 197
Amer N M and Jackson W B 1984 *Semiconductors and Semimetals* vol **21**, ed J I Pankove (New York: Academic) pp 85–111
Beerman H P 1967 *Am. Ceram. Soc. Bull.* **46** 737
Bosquet P 1971 *Spectroscopy and Its Instrumentation* (New York: Crane-Russack)
Christofides C, Engel A and Mandelis A 1990a *Ferroelectrics* (at press)
Christofides C, Mandelis A, Ghandi K and Wagner R E 1990b *Rev. Sci. Instrum.* (in press)
Coufal H and Mandelis A 1987 *Photoacoustic and Thermal Wave Phenomena in Semiconductors* ed A Mandelis (New York: North-Holland) p 149
Coufal H 1984a *Appl. Phys. Lett.* **44** 59
—— 1984b *Appl. Phys. Lett.* **45** 516
Kirev P 1975 *The Physics of Semiconductors* (Moscow: Mir) ch 8
Kynar 1983 *Piezo Film Technical Manual Pennwalt Corp.* King of Prussia, PA
Mandelis A 1984 *Chem. Phys. Lett.* **108** 388
Mandelis A, Wagner R E, Ghandi K, Baltman R and Dao P 1989 *Phys. Rev. B* **39** 5204
Mandelis A and Zver M M 1985 *J. Appl. Phys.* **57** 4421
Melles–Griot 1988 *Optics Guide (4) Technical Manual* pp 12–4
Roentgen W C 1914 *Ann. Phys., Lpz.* **45** 737
Rosencwaig A 1973 *Opt. Commun.* 7 305
—— 1980 *Photoacoustics and Photoacoustic Spectroscopy* (New York: Wiley-Interscience)
Tanaka K 1987 *Photoacoustic and Thermal Wave Phenomena in Semiconductors* ed A Mandelis (New York: North-Holland) ch 16
Tanaka K, Ichimara Y and Sindoh K 1988 *J. Appl. Phys.* **63** 1815
Wagner R E, Wong V K T and Mandelis A 1986 *Analyst* **111** 299
Wendlandt W W and Hecht H G 1966 *Reflectance Spectroscopy* (New York: Wiley)
Wilks P A Jr and Hirschfeld T 1968 *Appl. Spectrosc. Rev.* **1** 99
Wright G B (ed) 1969 *Light Scattering of Solids* (Berlin: Springer)
Yeou T 1938 *C.R. Acad. Sci., Paris* **207** 1042